

# Methane combustion dynamics in diabatic PSRs with detailed reaction mechanisms at low and high pressures

Francesco S. Marra and Luigi Acampora  
Istituto di Ricerche sulla Combustione - CNR  
Napoli, Italy

## 2 Introduction

Combustion phenomena very often, especially in industrial applications, involve an unsteady behavior, being intrinsically transient (f.i. ignition and explosions) or because affected by unsteady phenomena (like noise, turbulence, instabilities). The correct prediction of the unsteady behavior of a reactive mixture depends on a number of factors that change varying the operative conditions assumed. Thus, the unsteady combustion behaviors can depend upon transport mechanisms and their parameters[1, 2], but they are also affected by the time scales of the chemical kinetics[3]. Actually, in real configurations, these two class of effects share a wide overlapping of mutual interaction, being effectively separated only in limiting cases of very large or very low Damkohler numbers.

These considerations open the question about the ability of a selected reaction mechanism to include the relevant time scales governing the combustion dynamics. Of course, it is expected that detailed combustion mechanisms include all the real chemical time scales characterizing the combustion of a real fuel. Nevertheless, while developing such schemes, only one parameter is usually adopted to validate the resulting time scale with respect to an unsteady behavior, i.e. the Ignition Delay Time (IDT), while all other validations are assumed with respect to steady phenomena like jet stirred reactors and planar laminar flame propagation. However, the IDT represents the response of the system in a very particular configuration, running across a specific reaction path. It does not represent the effective combustion environment usually encountered by the reacting mixture when it faces an unsteady, possibly cyclic variation of temperature, composition and, in some cases, pressure. Therefore, the question about the capability of a given reaction mechanism to include the proper time scales in a wide range of unsteady conditions does not appear well assessed yet.

Not many studies have been performed in the past to include a more reliable assessment of the ability of chemical mechanisms to correctly reproduce unsteady behaviors, see f.i. [4, 5]. The Perfectly Stirred Reactor (PSR) appears a suitable compromise between simplicity of the archetypal reactor, allowing to really focus on the role of the chemical reactions, and the possibility to model a wide range of operating and environmental conditions [6].

Of course, to be effective, a validation procedure needs to be simple and capable to identify the most critical conditions, those in which the maximum discrepancies with the target value arise. This work develops trying to follow this path. A previous study [5] is extended to include different detailed mechanisms for methane-air combustion. Then, simulations are performed in key solution points where periodic solutions establish, spontaneously or by a forcing. Comparison of results allows to highlight several features of system dynamic response and their dependences upon the selected mechanism.

### 3 Model Description and Numerical Solution

We will make use of three different detailed kinetic schemes:

The *Gas Research Institute* mechanism (GRI), also known as GRIMEch [7], is one of the most widely used chemical kinetics mechanism for modelling methane and natural gas combustion in air. The current version (version 3.0) consists of 325 chemical reactions and 53 species.

The *San Diego* mechanism (SDG) describes C1-C4 oxidation and is designed to model a wide range of conditions from low to high temperature and pressure [8]. The philosophy underlying this mechanism is to include only a relatively small number of elementary steps that are of crucial importance to reproduce the target combustion phenomena. The version 2016-08-15 involves 269 reversible elementary reactions and 57 chemical species.

The *Politecnico di Milano* C1-C3 mechanism (PLM) developed by the Chemical Reaction Engineering and Chemical Kinetics group (CRECK) of the Politecnico di Milano [9] is a detailed mechanism of the pyrolysis, partial oxidation and combustion of hydrocarbon fuels up to 3 C atoms. In this work the version including both high and low temperature kinetic is adopted. This mechanism (version 1412, December 2014) consists of 107 species 2642 reactions.

The model equations of a time evolving diabatic PSR can be written as [6]:

$$\frac{dY_j}{dt} = \frac{Y_{j,f} - Y_j}{\tau} + \frac{W_j r_j}{\rho V}, \quad j = 1, 2, \dots, N_s \quad (1)$$

$$\frac{dT}{dt} = \frac{\sum_{j=1}^{N_s} Y_{j,f} (h_{j,f} - h_j)}{c_p \tau} - \frac{\sum_{j=1}^{N_s} h_j W_j r_j}{c_p \rho V} - \frac{\alpha S (T - T_{env})}{(c_p \rho V)} \quad (2)$$

Here  $t$ ,  $Y_j$ ,  $\tau$ ,  $W_j$ ,  $r_j$ ,  $\rho$ ,  $V$ ,  $N_s$ ,  $T$ ,  $h$ ,  $c_p$ ,  $\alpha$ ,  $S$  refer to time, mass fraction of specie  $j$ , residence time, molecular weight of species  $j$ , molar reaction rate of species  $j$ , density, reactor volume, number of species, temperature, specific enthalpy, constant pressure specific heat, heat loss coefficient and surface area of the reactor respectively. The subscript  $f$  refers to reactor feeding (inlet) conditions. Heat transfer to the wall depends on  $T_{env} = 300$  K and on the coefficient  $\alpha S/V = 125.4$  W m<sup>-3</sup> K<sup>-1</sup>. The residence time  $\tau$  is defined as  $\tau = (\rho V)/\dot{m}_f$  where  $\dot{m}$  is the mass flow rate.

Numerical integration of the ODE system given by 1-2 has been performed using the Cantera libraries to handle the chemical mechanisms and compute the reaction rates. Two ODE solvers, specifically `ode15s` by Matlab® and `radau5` [10] were adopted. Errors were controlled using always a relative tolerance of  $1 \times 10^{-8}$  and an absolute tolerance of  $1 \times 10^{-12}$ . An efficient numerical tool for the continuation of detailed mechanisms, developed by the same authors [11, 12] was adopted for the parametric continuation analyses.

#### 4 Combustion dynamics in PSRs.

Methane-air (air composition: O<sub>2</sub> 21%, N<sub>2</sub> 79% by volume) mixtures adopted are: a lean (equivalence ratio  $\phi = 0.5$ ), the stoichiometric and a rich mixture ( $\phi = 2$ ). Two values of the pressure, atmospheric pressure and a much higher pressure of 50 atm, are investigated. Solution maps, and then different forcing mechanisms, can be built with respect to different parameters. In this work only the nominal residence time, i.e. the inlet mass flow rate, is considered as continuation parameter.

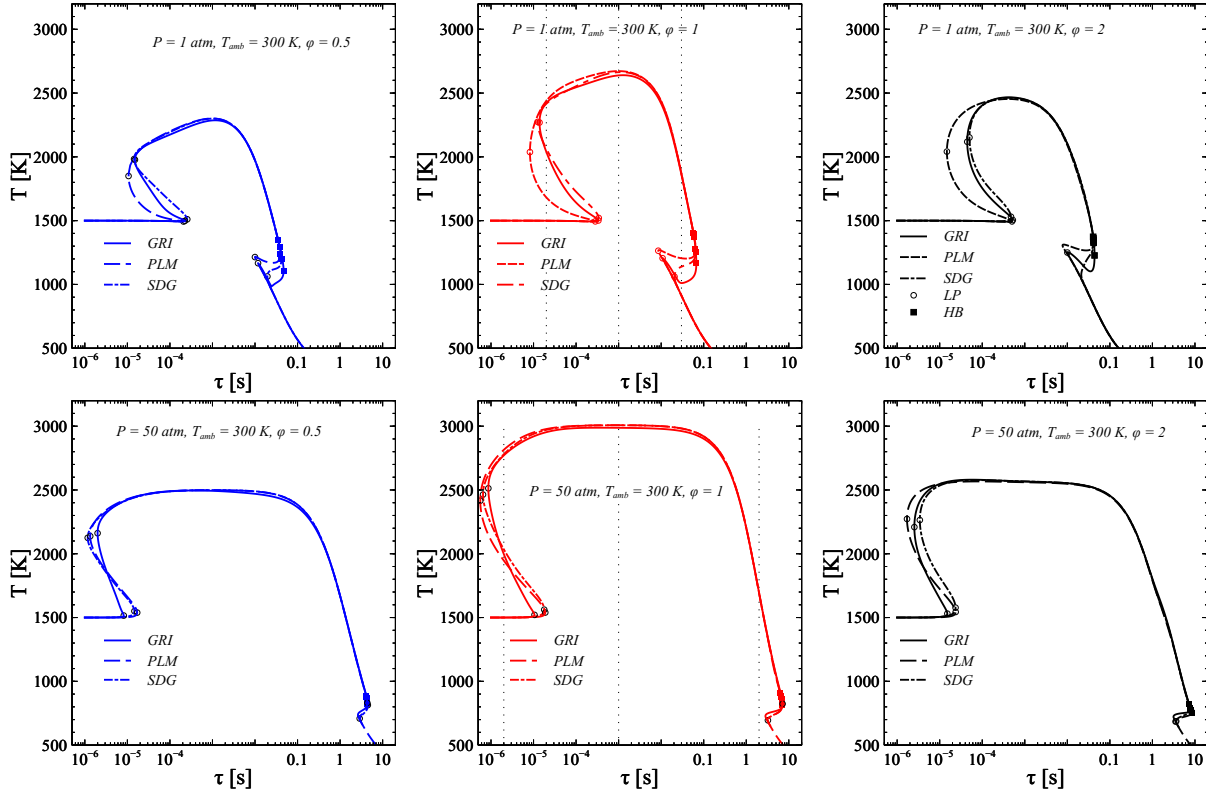


Figure 1: Solutions maps in terms of temperature vs residence time: methane-air mixture at three different values of  $\phi$ ,  $T_{in} = 1500\text{ K}$  and  $T_{amb} = 300\text{ K}$ . Top  $P = 1\text{ atm}$ , bottom  $P = 50\text{ atm}$ . Comparison of the GRI, PLM and SDG.

The solution maps reported in Figure 1 allow a comparison of the three different selected detailed mechanisms. The first observation that immediately arises is the very large discrepancy on the extinction points, especially for the PLM mechanisms at low pressure. For this mechanism the extinction point shifts significantly towards lower values both in terms of the limit residence time of extinction and the corresponding temperature. At low pressure, the GRI and the SDG looks similar along all the stable branches. The results at high pressure are different, all extinction points differs and without any determined order, probably indicating that no well assessed reference points are available in this conditions.

The stoichiometric mixture has been perturbed at three different values of  $\tau_{nom}$ , selected to identify steady and stable solution points identified in Fig. 1 by the vertical dotted lines drawn at  $\tau_{nom} = \{2 \times 10^{-5}, 1 \times 10^{-3}, 3 \times 10^{-2}\}$  s for  $P = 1\text{ atm}$ , and  $\tau_{nom} = \{2 \times 10^{-6}, 1 \times 10^{-3}, 2\}$  s for  $P = 50\text{ atm}$ , not all discussed here. Three different frequencies are compared: assuming  $1/\tau_{nom}$  the nominal frequency at a given nominal

residence time, two other frequencies are considered, an higher frequency given by  $10/\tau_{nom}$  and a lower frequency given by  $1/(10\tau_{nom})$ . Two different amplitudes are also compared,  $A = 0.05$  and  $A = 0.2$ .

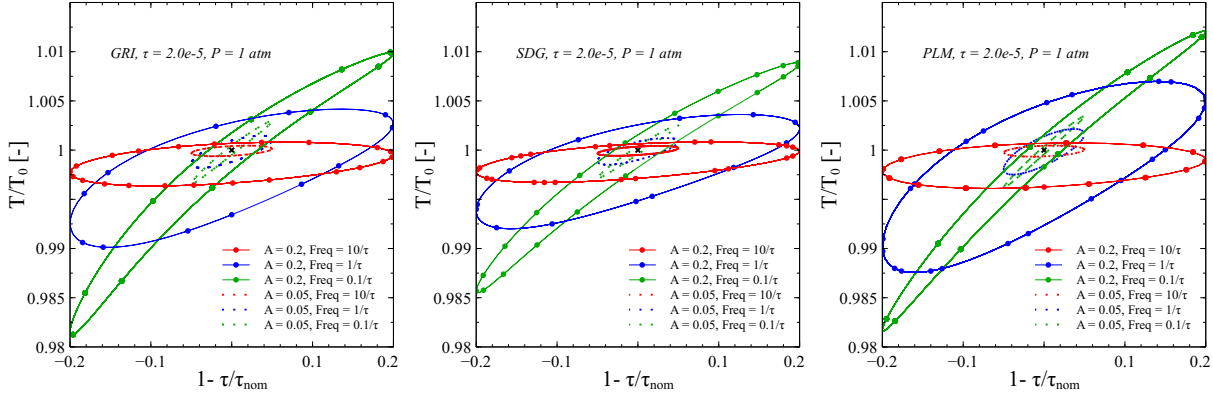


Figure 2: Phase plots of harmonically forced solutions: temperature vs forcing amplitude. Stoichiometric methane-air mixture,  $P = 1 \text{ atm}$ ,  $\tau = 2e - 5 \text{ s}$ . From left to right GRI, SDG and PLM.

The first condition analyzed is  $P = 1 \text{ atm}$  and  $\tau_{nom} = 2 \times 10^{-5} \text{ s}$ . Here the dynamics response to harmonic forcing, illustrated in Fig. 2, is very similar for the three mechanisms, despite we are close to the extinction point where the three mechanisms shows the largest discrepancies of the equilibrium maps. Amplitudes have the same order of magnitude (a little larger for PLM), progressively varying with the frequency, even if the orbits of GRI and SDG at  $f = 1/\tau_{nom} \text{ s}^{-1}$  are closer to the orbit at  $f = 10/\tau_{nom} \text{ s}^{-1}$ . Not significant discrepancies are observed for the phase shift that, increasing the frequency, increases from 0 to 90 degree.

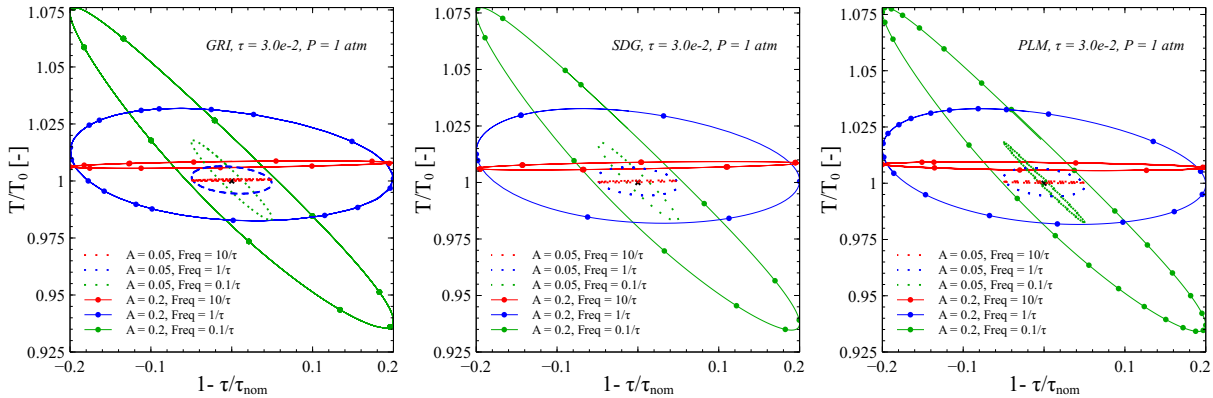


Figure 3: Phase plots of harmonically forced solutions: temperature vs forcing amplitude. Stoichiometric methane-air mixture,  $P = 1 \text{ atm}$ ,  $\tau = 3 \times 10^{-2} \text{ s}$ . From left to right GRI, SDG and PLM.

Moving at the longer residence time, see Fig. 3, all signals for every mechanism, at each frequency and amplitude of forcing are almost identical: in these conditions, chemistry is anymore the driving effect, so that the system response depends upon the other acting mechanisms, the heat losses, acting totally the same independently from the chemical mechanism adopted.

The selected residence time  $\tau_{nom} = 2 \times 10^{-6}$  at  $P = 50 \text{ atm}$ , locates a condition where all the three profiles of equilibrium points run coincident or parallel (at little higher values the PLM mechanism). As a consequence, no differences are expected in the orbits of harmonically forced signals. This is confirmed by

the comparison of plots reported in Fig. 4. Just the amplitude of the PLM signals results slightly higher, because of the larger perturbation of the effective residence time induced by the higher temperature.

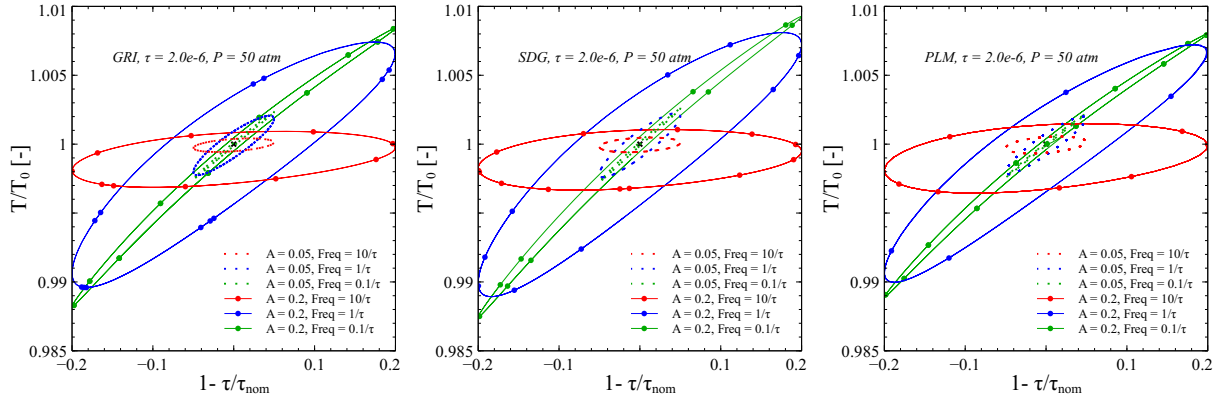


Figure 4: Phase plots of harmonically forced solutions: temperature vs forcing amplitude. Stoichiometric methane-air mixture,  $P = 50 \text{ atm}$ ,  $\tau = 2 \times 10^{-6} \text{ s}$ . From left to right GRI, SDG and PLM.

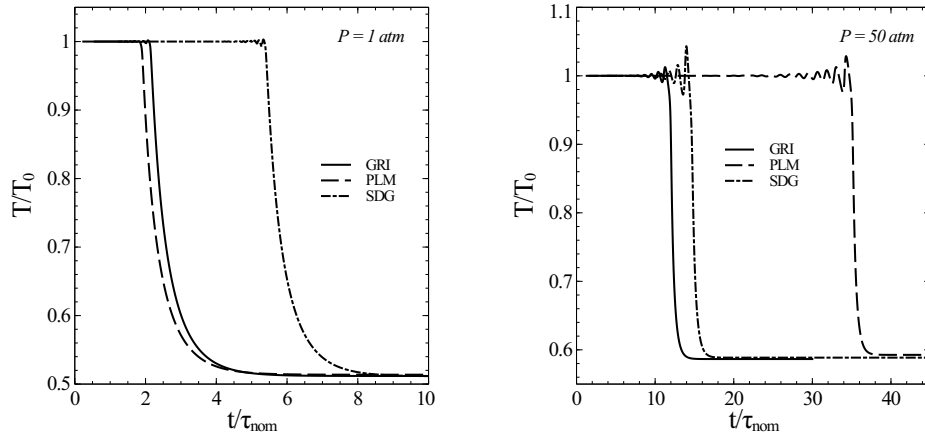


Figure 5: Spontaneous evolution of the solution for initial conditions very close to the first Hopf bifurcation. Stoichiometric methane-air mixture,  $P = 1 \text{ atm}$  (left) and  $P = 50 \text{ atm}$  (right) adopting the GRI, PLM and SDG.

Fig. 5 reports the result of simulations performed starting from the equilibrium point following the Hopf bifurcation computed by the continuation analysis for each mechanism. It results that when the oscillations start to develop, the solution become unstable so that the equilibrium drops to the lower stable branch. However, the times required by the three different mechanisms to move from the initial point to the new stable conditions are quite different for each mechanism.

## 5 Conclusions

It has been shown that a preliminary investigation of the equilibrium solution of a PSR is able to give guidance on the effect that the adoption of a particular chemical mechanism can have when the PSR is subject to harmonically forced perturbation. Significant differences can results even comparing detailed

mechanisms, which are expected to include almost all the relevant time scales of a specific combustion system. Macroscopic differences arise in the bifurcation diagram in regions where chemical kinetics is predominant with respect to heat losses. These differences influence especially the phase shift in response to harmonic forcing, that shows a strong dependence upon the frequency of the forcing applied.

Investigation of the dynamic behavior in points where instabilities develop because of the coupling between heat losses and chemical kinetics reveal that these are location of maximum discrepancies in the prediction given by the different detailed mechanisms.

## References

- [1] Cho JH., Lieuwen T. (2005). Laminar Premixed Flame Response to Equivalence Ratio Oscillations. *Combust. Flame* 140: 116.
- [2] Di Sarli V., Di Benedetto A., Marra FS. (2008) Influence of system parameters on the dynamic behaviour of an LPM combustor: Bifurcation analysis through CFD simulations. *Combust. Theor. Model.* 12: 1109.
- [3] Law CK. (2005). Comprehensive description of chemistry in combustion modeling. *Combust. Sci. Technol.* 177: 845.
- [4] Sidhu HS., Forbes LK. Gray BF. (1997). Forced reaction in a CSTR: a comparison between the full system and the reduced model. *Chem. Eng. Sci.* 52: 2667.
- [5] Marra FS., Acampora L., Martelli E. (2015) Non-linear response to periodic forcing of methane-air global and detailed kinetics in continuous stirred tank reactors close to extinction conditions. *Int. J. Spray Combust.* 7: 175.
- [6] Glarborg P., Miller JA., Kee RJ. (1986). Kinetic modeling and sensitivity analysis of nitrogen oxide formation in well-stirred reactors. *Combust. Flame* 65: 177.
- [7] Smith GP., Golden DM., Frenklach M., Eiteener B., Goldenberg M., Bowman CT., Hanson RK., Gardiner WC., Lissianski VV., Qin ZW. (2000). *Gri-mech 3.0*.
- [8] Prince JC., Treviño C., Williams FA. (2017). A reduced reaction mechanism for the combustion of n-butane. *Combust. Flame* 175: 27.
- [9] Ranzi E., Frassoldati A., Grana R., Cuoci A., Faravelli T., Kelley A., Law CK. (2012) Hierarchical and comparative kinetic modeling of laminar flame speeds of hydrocarbon and oxygenated fuels. *Prog. Energ. Combust.* 38: 468.
- [10] Hairer E. Wanner G. (1999). Stiff differential equations solved by Radau methods. *J. Comput. Appl. Math.* 111: 93.
- [11] Acampora L. Marra FS. (2015). Numerical strategies for the bifurcation analysis of perfectly stirred reactors with detailed combustion mechanisms. *Comput. Chem. Eng.* 82: 273.
- [12] Acampora L., Mancusi E., Marra FS. (2015). Bifurcation analysis of perfectly stirred reactors with large reaction mechanisms. *Chem. Engineer. Trans.* 43: 877.